Influence of the grafting process on the orientation and the reactivity of azide-terminated monolayers onto silica surface

Nisreen Al-Hajj, Yannick Mousli, Antoine Miche, Vincent Humblot, Julien Hunel, Karine Heuze, Thierry Buffeteau, Emilie Genin, Luc Vellutini

Influence of the grafting process on the orientation and the reactivity of azide-terminated monolayers onto silica surface

Nisreen Al-Hajj[a,b], Yannick Mousli[a,b], Antoine Miche[c], Vincent Humblot[c,d], Julien Hunel[a,b], Karine Heuzé[a,b], Thierry Buffeteau[a,b], Emilie Genin[a,b,*], Luc Vellutini[a,b,*]

[a] *Univ. Bordeaux, ISM, UMR-5255, F-33405 Talence, France*
[b] *CNRS, ISM, UMR5255, F-33405 Talence, France*
[c] *Sorbonne Université, Centre National de la Recherche Scientifique, Laboratoire de Réactivité de Surface (LRS), UMR CNRS 7197, Paris F-75252, France*
[d] *FEMTO-ST Institute, UMR CNRS 6174, Université Bourgogne Franche-Comté, 15B avenue des Montboucons, 25030 Besançon Cedex, France*

Click chemistry is widely used in materials and surface science for its high efficiency, ease of use and high yields. Azide-terminated SAMs have been prepared successfully by using three different deposition methods (post-functionalization and direct grafting by immersion as well as spin coating). Strikingly, our study shows that the reactivity of the azido group on the surface with the alkyne in solution is not trivial and seems to be closely related to the orientation of the azide. Indeed, more the azide is vertically oriented more it is accessible and reactive. The orientation of azido dipoles at the surface depends strongly on the method used to prepare the monolayer. The post-functionalization method allows to have a homogeneous population of the azide groups on the surface with a better vertical orientation than that obtained using direct grafting by immersion or spin coating processes. Whatever the type of azide-terminated SAMs, the reactivity of the accessible vertical azido groups is complete. This study clearly demonstrates that it is possible to control the amount of reactive azides and, consequently, the amount of molecules immobilized on the surface after the click reaction by choosing the deposition method.

1. Introduction

Surface chemistry plays a crucial role in material sciences to control the functionalization at the solid–liquid interface in the field of biosensors and biochips [1–4]. The interface functionalization confers the physico-chemical properties to the surface of the planar solid support such as the wettability [5], bioadhesion [6], antifouling [7], etc. For a diagnostic platform, the sensitivity, the selectivity and the rate of response are directly related to the quality of the biomolecule's immobilization in terms of the amount, the orientation and the nature of the linkage with the surface (covalent or non-covalent) [8,9].

The covalent chemical modification of oxide surfaces with a molecular level control can be achieved thanks to self-assembled monolayers (SAMs) [10]. The use of a silylated coupling agent is one of the most efficient methods to prepare functionalized monolayers on oxide (silica for example) surfaces [11,12]. The biomolecule's immobilization (conjugation reaction) strategies often use non-selective methods involving either physisorption or random covalent bonds on functionalized SAMs which can induce a lack of bioactivity.

The regioselective and bioorthogonale copper-catalyzed alkyne-azide cycloaddition reaction (CuAAC) constitutes an interesting way to covalently immobilize, *via* a specific ligation site, biomolecule species, and thus control their orientation onto the surface [13–15]. The bioorthogonal group (azide or alkyne) is introduced in the biomolecules of interest through metabolic, enzymatic labeling or using synthetic methods. This click reaction allows the modification of surfaces with stable bonds in a selective and efficient way since the azide-alkyne cycloaddition reaction is quantitative, rapid, chemoselective and pH independent [16]. This coupling method using soft conditions often prevents incomplete surface functionality conversion and side reactions, allowing a fine control of the chemical composition at the material interface.

The azide-terminated SAMs onto silica can be achieved by two main approaches. The most used is the post-functionalization method involving the replacement of the terminal bromine atom by an azide group *via* a nucleophilic substitution [17–27]. The conversion yields of bromine into azide vary from 80 to 100%, depending on the quality of the monolayers [22,28]. The packing density can interfere with the

preferred SN_2 transition state requiring backside attack of the incoming nucleophile, which may lead to an incomplete conversion caused by steric hindrances. Mixed self-assembled monolayers of bromo- and alkylsilanes can be used to adjust the density of azide terminal groups. However, the composition of the mixed SAMs depends strongly on the experimental conditions used for the grafting process showing a preferential surface adsorption or not of the bromosilane [29,30]. A complete substitution was achieved when the bromine-terminated silane is at least one methylene unit longer than the methyl-terminated silane, suggesting that bromine end groups are less sterically hindered [31]. In contrast, the substitution yield is 80% when the two silylated compounds have the same alkyl chain length [24]. Finally, the density of azide groups on the surface can be controlled kinetically by an appropriately timed quenching of the substitution reaction of pure bromo-terminated SAMs, leading to monolayers with azide groups randomly distributed [23]. This last method for mixed SAMs elaboration prevents preferential surface adsorption and phase separation.

Another possibility of post-functionalization method consists of derivatizing amino-terminated monolayers [32,33]. For example to have aryl azides surfaces, the efficiency of the azidification ranges from 30% to 90% below the reported 93% for the solution-phase reaction [34,35]. The steric effect seems to prevent a complete surface azidification. This study also shows that the efficiency of the triazole formation depends on the density of the azide groups on the surface. Indeed, the cycloaddition seems more favorable for low azide density because sites that have already reacted do not reduce the accessibility of other azide groups. This post-modification strategy which potentially generates unreacted functional groups can be avoided by directly incorporating the aryl azide silylated compound into the monolayer to afford a mixed SAMs while controlling the surface ratio of different reactive groups and so improving their accessibility and reactivity [36].

The second way to obtained pure azide-terminated SAMs consists in the direct grafting of the pre-synthesized azido silylated coupling agent. Generally, commercially available organosilanes such as 11-azidoundecyltrimethoxysilane and *p*-azidomethylphenyltrimethoxysilane [37] were used to prepare azide-terminated SAMs. Recently, we have reported a versatile synthetic methodology to prepare various azido-silylated coupling agents using the platinum-catalyzed hydrosilylation of stable olefinic precursors bearing an azide group [38]. This new possibility opens the way to obtain new azide-terminated monolayers with modular composition and structure, leading to original physicochemical properties. There are few examples of the preparation of azide-terminated SAMs onto silica surface by the direct grafting of azido-silylated compounds using the conventional deposition methods such as solution immersion [37,39–42] and chemical vapor deposition [43,44]. Only one example describes the deposition of an azide-terminated monolayer by the Langmuir-Blodgett technique [45]. Recently, we have successfully prepared an azide-terminated SAM by using the spin coating technique in ambient atmosphere [38]. This is an interesting alternative process that is fast, simple, easy to handle and requires less solvent.

From a general point of view, the chemical reactions at the solid/solution interfaces are well-known to be more difficult than the reactions in solution. This behavior can be due to the solvation effects, transport limitations, charge and dipole effects, and steric constraints. The success of the reaction depends strongly on the reactivity and accessibility of the functional end group on the monolayers toward the reactant from the solution.

This work describes a comprehensive study regarding the self-assembly of the resulting 11-azidoundecyltrimethoxysilane onto silica surfaces, along with the influence of the grafting methods (post-functionalization, direct grafting by immersion and spin coating processes) on the orientation and the reactivity of the terminal azide groups (Scheme 1). Understanding the behavior of the azide group in pre-functionalized surfaces allows us to improve its reactivity with biomolecules. Chemical modifications of the surfaces have been investigated using Polarization Modulation Infrared Reflection Adsorption Spectroscopy (PM-IRRAS) and X-ray Photoelectron Spectroscopy (XPS). Atomic Force Microscopy (AFM) was also used to image the surface topography. We thus present the first systematic study of azido-terminated SAMs prepared by direct grafting (Scheme 1b) *via* several methods in comparison to the classical post-functionalization process (Scheme 1a). Significant differences have been highlighted in terms of azide orientation and consequently in terms of reactivity *via* click chemistry, as illustrated by the Scheme 1.

2. Experimental section

2.1. Substrate preparation

The SiO_2/Au substrates were supplied by Optics Balzers AG. They correspond to Goldflex mirror with SiO_2 protection layer (GoldflexPRO, reference 200785). Their absolute reflectance was higher than 98% in the 1.2–12 μm spectral range. The thickness of the SiO_2 layer, measured by ellipsometry, was 215 ± 7 Å, using a refractive index of 1.46 (Ielli2000 NFT ellipsometer, $\lambda = 532$ nm). A homogeneous surface was observed by atomic force microscopy (AFM) with a root mean square (rms) roughness of 9 Å (Thermomicroscope Autoprobe CP Research, Park Scientific).

Before each surface functionalization, the SiO_2/Au substrates were washed with Milli-Q water (18 MΩ.cm), sonicated in chloroform for 15 min, activated by UV-ozone (185–254 nm) for 30 min, introduced immediately into the silanization flask, let under reduced pressure for 1 h 30 and then stored under argon atmosphere.

2.2. Formation of Self-Assembled Monolayers (SAMs)

2.2.1. Azide monolayer preparation by the post-functionalization method, ***SAM1***

Bromine terminated monolayers using 11-bromoundecyltrimethoxysilane. A solution of freshly prepared 11-bromoundecyltrimethoxysilane (0.05 mmol) in dry chloroform (50 mL) was prepared in a schlenk flask under argon atmosphere. A solution of trichloroacetic acid (TCA) (0.8 mg, 5.10^{-6} mol) in dry chloroform (50 mL) was prepared in another schlenk flask under argon atmosphere. Dry chloroform (100 mL), the silylated compound solution and then the TCA solution were successively added in the silanization flask at 20 °C. The substrates were kept immersed under argon atmosphere for 16 h at 20 °C. They were washed by sonicating in toluene (2 × 5 min), chloroform (2 × 5 min), water and chloroform (2 × 5 min), respectively, and dried under nitrogen flow.

Nucleophilic substitution of bromide with azide. The bromine terminated monolayers were immersed in a saturated solution of sodium azide in dry DMF for 48 h at room temperature under argon atmosphere. The substrates were subsequently sonicated for several minutes in DMF, water and chloroform, respectively, and dried under nitrogen flow. The success of the Br displacement was confirmed by XPS looking at the Br 3d peak.

2.2.2. Azide Monolayer preparation by direct grafting method, ***SAM2***

A solution of freshly prepared 11-azidoundecyltrimethoxysilane (0.05 mmol) in dry chloroform (50 mL) was prepared in a schlenk flask under argon atmosphere. A solution of trichloroacetic acid (TCA) (0.8 mg, 5.10^{-6} mol) in dry chloroform (50 mL) was prepared in another schlenk flask under argon atmosphere. Dry chloroform (100 mL), the silylated compound solution and then the TCA solution were successively added in the silanization flask at 20 °C. The substrates were kept immersed under argon atmosphere for 16 h at 20 °C. They were washed by sonicating in toluene (2 × 5 min), chloroform (2 × 5 min), water and chloroform (2 × 5 min), respectively, and dried under nitrogen flow.

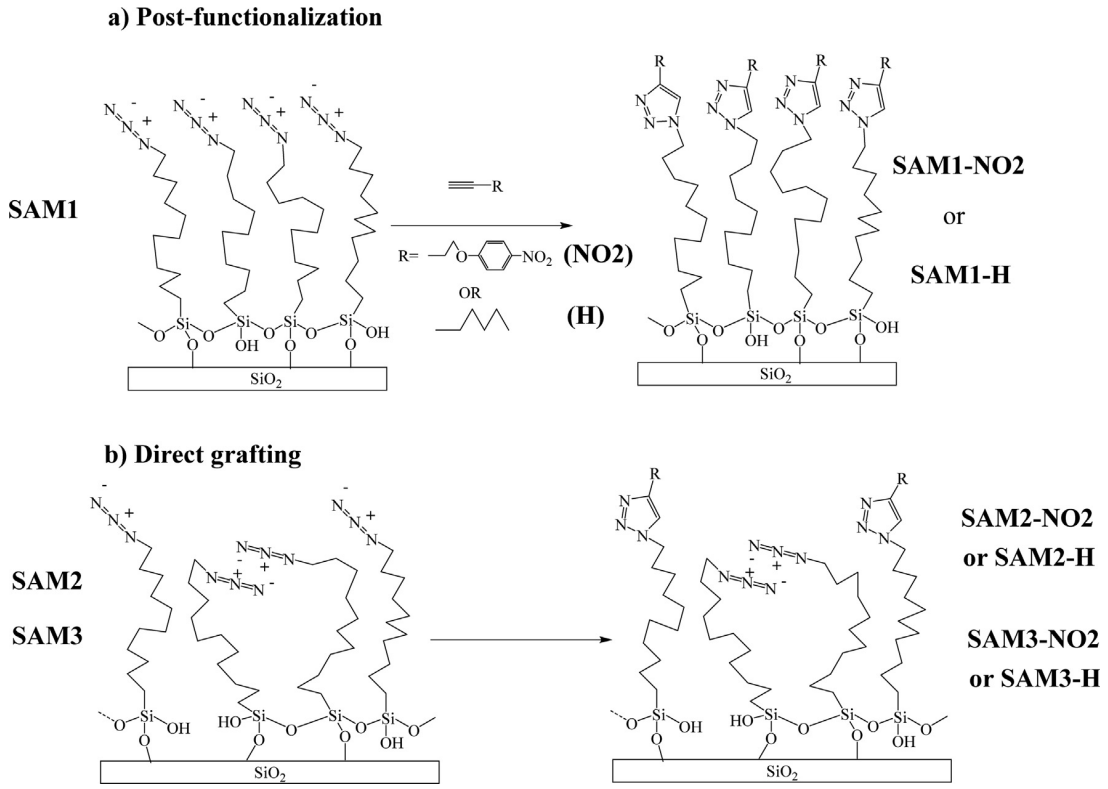

Scheme 1. Left) Schematic representation of the molecular organization inside the **SAM-N3** depending of the deposition methods: a) by post-functionalization from SAM-Br (**SAM1)** and b) by the direct grafting of silylated coupling agent (**4**) by immersion (**SAM2**) and spin coating (**SAM3**) processes. Right) Schematic representation of the corresponding SAMs after click reaction with the nitro probe (**SAMx-NO2**) and the heptyne compound (**SAMx-H**).

*2.2.3. Azide Monolayer preparation by spin coating method, **SAM3***

Freshly prepared 11-azidoundecyltrimethoxysilane was dissolved in dry chloroform HPLC grade under inert atmosphere to prepare a solution at 4×10^{-3}M. 40 µL of this freshly prepared solution of organosilane was used to spin coat the substrate (rotated at 6000 rpm for 40 s). The sample was dried at ambient temperature for 30 min in a laminar flow hood, then washed by sonicating in chloroform (2×5 min) and dried under nitrogen flow.

2.2.4. Click reaction of azide substrates and alkynes

1,3-dipolar cycloaddition reactions were carried out in a steriplan soda-lime petri dish (diameter: 60 mm; height: 15 mm) under inert atmosphere by immersing the azide terminated substrate in a mixture of degassed Milli-Q water (6.36 mL) and degassed DMSO (1.35 mL) followed by the addition of three solutions respectively : the solution of alkyne (heptyne or nitro probe) in degassed DMSO (0.25 mL, 0.0036 M), the solution of copper catalyst in degassed Milli-Q water (7.1 µL, 0.0125 M) and the solution of sodium ascorbate in degassed Milli-Q water (35.5 µL, 0.01 M). The sample was stirred overnight under inert atmosphere in the dark at ambient temperature by using an orbital shaker, and then sonicated in DMSO (5 min), Milli-Q water (2×5 min), ethanol 95% (2×5 min), chloroform (2×5 min) and dried under nitrogen flow.

2.3. Surface characterization

AFM measurements. AFM height images of SAMs on SiO_2/Au substrates were performed on a Bruker's Dimension Icon Atomic Force Microscope (AFM) system in PeakForce QNM® mode (Quantitative Nanomechanical Mapping) with ScanAsyst-Air tips (APEX = 2 nm, spring constant k = 0.4 N/M). The AFM height images are representative of three different areas.

PM-IRRAS experiments. PM-IRRAS experiments were performed on a ThermoNicolet Nexus 670 FTIR spectrometer equipped with a PM-IRRAS optical bench, following the experimental procedure previously published [46,47]. The PM-IRRAS spectra were recorded at a resolution of 4 cm^{-1} during 4 h acquisition time. The PM-IRRAS spectra were calibrated in order to be presented in IRRAS units [47,48]. All spectra were collected in a dry-air atmosphere after 30 min of incubation in the chamber. All spectra in the figures are average of at least 4 spectra.

X-ray Photoelectron Spectroscopy (XPS) experiments. XPS analyses were performed using an Omicron Argus X-ray photoelectron spectrometer, equipped with a monochromated AlK_α radiation source ($h\nu$ = 1486.6 eV) and a 280 W electron beam power. The emission of photoelectrons from the sample was analyzed at a take-off angle of 45° under ultra-high vacuum conditions ($\leq 10^{-10}$ Torr). For the molecular compounds (powders embedded in an indium foil) a flood gun was used in order to compensate the charging effect of the insulating powder. Spectra were recorded with a 100 eV pass energy for the survey scan and 20 eV pass energy for the C1s, O1s, N1s, Si2p regions. Binding energies were calibrated against the C1s binding energy at 285.0 eV and element peak intensities were corrected by Scofield factors [49]. The peak areas were determined after subtraction of a Shirley background. The spectra were fitted using Casa XPS v.2.3.15 software (Casa Software Ltd., U.K.) and applying a Gaussian/Lorentzian ratio G/L equal to 70/30.

3. Results and discussion

3.1. Effects of the deposition methods on azide orientation

Azido-terminated monolayers (**SAM-N3**) immobilized onto silica substrate were prepared by using three different methods of deposition. **SAM1** was prepared by the post-functionalization method from 11-

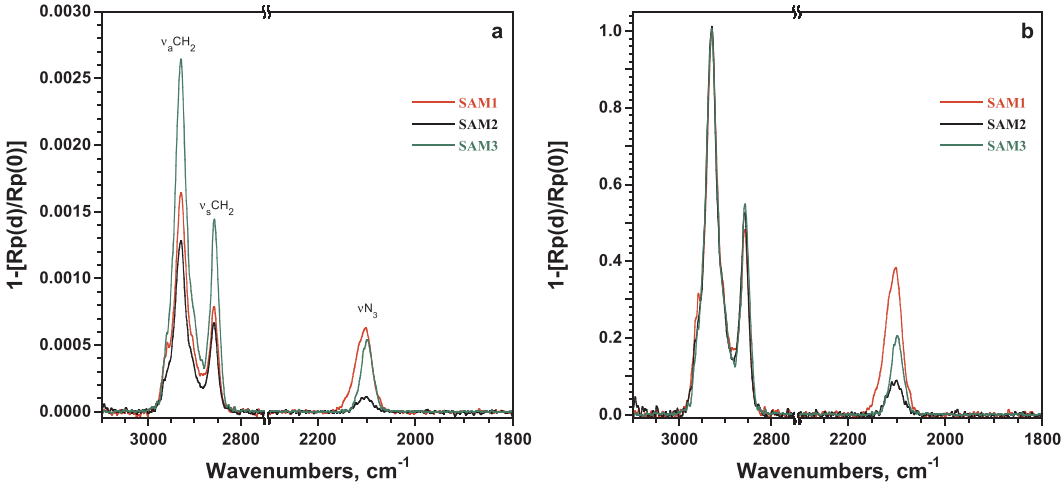

Fig. 1. a) Non normalized and b) normalized PM-IRRAS spectra of **SAM-N3** grafted onto SiO_2/Au substrate depending on the deposition processes in the 3100–1800 cm^{-1} spectral range. For b), spectra are normalized with respect to the methylene band at 2928 cm^{-1}.

bromoundecylsiloxane monolayers (SAM-Br). **SAM2** and **SAM3** were obtained by the direct grafting of the pre-synthesized 11-azidoundecyltrimethoxysilane **4** (Supporting information), by using the conventional solution immersion method (**SAM2**) and the spin coating technique (**SAM3**).

After their deposition the azido-terminated monolayers were analyzed by PM-IRRAS. Fig. 1a shows the PM-IRRAS spectra of **SAM-N3** in the 3100–1800 cm^{-1} region, related to the stretching modes of the methylene groups (3000–2800 cm^{-1}) and to the stretching mode of the terminated azide group (around 2100 cm^{-1}). The functionalization of the substrate by an alkylazide monolayer was confirmed by PM-IRRAS measurements which reveal the presence of the antisymmetric (ν_aCH_2) and symmetric (ν_sCH_2) stretching modes of the methylene groups as well as the asymmetric stretching (ν_aN_3) mode of the azide groups for the three deposition methods. The ν_aN_3 band of the azide terminal groups is observed close to 2100 cm^{-1} for all the alkylazide monolayers. The wavenumbers of the antisymmetric (ν_aCH_2) and symmetric (ν_sCH_2) stretching modes of methylene groups are sensitive to both the conformation (*gauche* or *trans*) and the order of the alkyl chains. The ν_aCH_2 and ν_sCH_2 bands are observed at 2928 cm^{-1} and 2857 cm^{-1}, respectively, for all the azide monolayers, revealing a disorder of the alkyl chains in the monolayers. These observations are consistent with a liquid-like state due to the short *n*-alkyl chain lengths, the Si-O-Si distances of the anchoring groups and the large size of azide terminal groups [50].

The intensities measured on the PM-IRRAS spectrum of **SAM3** for the antisymmetric (ν_aCH_2) and symmetric (ν_sCH_2) stretching modes of the methylene groups (i.e. 0.0027 and 0.0015, respectively) are similar to those measured for azide-terminated thiol monolayer ($N_3C_{12}H_{24}SH$) deposited on gold substrate [51]. Thus, these intensities of the ν_aCH_2 and ν_sCH_2 bands observed in Fig. 1a are consistent with the formation of a single monolayer on the silica surface. For **SAM1** and **SAM2** the intensities of the methylene bands are weaker than for **SAM3**, which corresponds to less matter on the surface, suggesting less densely packed monolayers and/or much thinner monolayers. The AFM images of **SAM-N3** show homogeneous organic layers without the presence of defaults (holes, aggregates…), revealing a uniform grafting process on the whole surfaces (Supporting information, Fig. S1). An estimation of the monolayer's thickness has been performed for the three **SAM-N3** systems by simulating the PM-IRRAS spectra at various thicknesses using the isotropic optical constants of **4**. The optical constants (refractive index and extinction coefficient) of **4** have been determined in the infrared spectral range from polarized attenuated total reflectance (ATR) spectra using a known procedure (Supporting information, Figs. S2a and S2b) [52,53]. The linear dependence of the IRRAS intensity of the ν_aCH_2 mode with the monolayer thickness (Supporting information, Fig. S3) allowed us to find 15.0, 9.3 and 7.3 Å for **SAM3**, **SAM1** and **SAM2**, respectively. It is noteworthy that these values only make sense if the packing of the three monolayers is the same as for the layer deposited onto the ATR crystal. Indeed, the decrease of the ν_aCH_2 intensity on PM-IRRAS spectra can also be due to less densely packed monolayers with similar thicknesses. These calculated thicknesses are lower than the theoretical length of the **4** silane with an all-*trans* conformation of the alkyl chains (which is approximately 19 Å) [54]. In the literature, the thickness of the azide monolayers varied in a wide range of 7 Å to 19 Å, according to the deposition method and experimental conditions [25,34,39,40]. For **SAM3** the higher value can be explained by the spin coating process where two phenomena act simultaneously, the spin and the evaporation at the ambient atmosphere [55]. At the early stage of spinning the liquid drop spreads homogeneously over the whole surface and evaporation increases the concentration which promotes the fast adsorption of **4** on the wetting surface; inducing the crosslinkage of molecules to afford a highly dense monolayer. In contrast, **SAM1** and **SAM2** are much thinner due to the solution immersion method which uses a low concentration of molecules. The rate of hydrolysis of the silylated compound, which depends on the leaving group, is known to play an important role in the structure of the SAM [56]. The assembly of the monolayers in diluted solution using anhydrous solvent requires several hours due to the lower rate of hydrolysis of the trimethoxysilyl groups. The slow incorporation of the molecules inside the layer and the steric constraints limit the saturation density which induces a greater mobility and tilting of the chains responsible for a sparsely packed SAM. Depending on the orientation of the chains, the thickness should be equal to or less than the molecular chain length (1.9 nm) of compound **4**, which is consistent with the calculated thicknesses. As alkyl chains are disordered in all types of **SAM-N3**, we consider that the behavior of alkyl chains is similar for the three grafting processes, and the corresponding PM-IRRAS spectra have been normalized with respect to the ν_aCH_2 band. The normalized PM-IRRAS spectra (Fig. 1b) revealed significant differences in the intensity of the azide band, according to the deposition methods. The intensity of the ν_aN_3 band with respect to the ν_aCH_2 band decreases in the order **SAM1** > **SAM3** > **SAM2**. This behavior is certainly due to the different packing density of monolayers which could affect how the adjacent azide groups interact each other, inducing different orientations of the dipoles. Due to the surface selection rule of PM-IRRAS on metallic surfaces (the intensity of a band is zero for a transition moment parallel to the surface and is maximum for a transition moment perpendicular to

the surface), the different intensities of azide bands may be attributed to an orientation effect of this dipole which can explain the nonlinear relationship between the azide and the methylene bands [57]. These results suggest a preferential parallel orientation of the azide group, with a decrease of the tilt angle (with respect to the normal surface) in the order **SAM2** > **SAM3** > **SAM1** [39]. By using the optical constants of azide mode (k_{max} = 0.261 at 2100 cm^{-1}) and calculating the IRRAS intensity of this mode for different orientations of the ν_aN_3 dipole from 0° (perpendicular to the surface) to 90° (parallel to the surface) using an uniaxial orientation, we found mean orientation values of 78°, 70.5° and 63° for **SAM2**, **SAM3** and **SAM1**, respectively (Supporting information, Fig. S4). The fact that the ν_aN_3 dipoles orientate more parallelly to the surface for less densely packed monolayer is certainly related to the presence of dipole–dipole interactions within the monolayer.

XPS experiments were carried out on the different **SAM-N3** in order to confirm the presence of the azido groups and to obtain more information about their organization. First, XPS spectrum of compound **4** was measured in the N1s region to acquire spectral reference of the azido group (Supporting information, Fig. S5a). It shows the presence of two well defined contributions : one at low binding energies (BE), centered at 401.2 ± 0.1 eV and composed of two overlapped peaks, corresponding to the nitrogen atoms linked to the alkyl chain (=N-), and to the electron enriched one at the end of the azido group ($^{-}$N =); the second contribution at higher BE (405.0 ± 0.1 eV) is assigned to the electron deficient nitrogen atom (=N^{+}=) in the middle of the azido group. A ΔBE = 3.8 eV is observed, with a higher intensity of the low BE component, which is in very good agreement with what is usually observed in the literature for azido groups [34,58].

Fig. 2 presents XPS spectra of **SAM-N3** surfaces in the N1s region for the three different methods of deposition. The XPS spectra of **SAM1** is quite different than those of **SAM2** and **SAM3**, despites the fact that the three SAM compositions are identical. In Fig. 2a, corresponding to the post-functionalized **SAM1**, the N1s profile is identical to the one observed for azido compound **4** in Fig. S5a, with two contributions separated by around 4 eV, and with a higher intensity of the low BE component. In contrast, the XPS spectra obtained for both direct grafting of SAMs, presented in Fig. 2b (**SAM2**) and 2c (**SAM3**), reveal a different N1s profile: first, the high BE peak at around 405 eV is weaker than for **SAM1**, and the contribution at lower BE is broader and could be fitted with at least three contributions, in opposition of the two observed for **SAM1**. The extra contribution appears at 1 eV higher than the two other ones, and is likely due to the central nitrogen atom (=N^{+}=) in dipole–dipole interactions with neighboring azido groups. Such interactions involve antiparallel orientation of azido groups with sharing electrons, resulting in the energy shifts observed in Fig. 2b and 2c.

The PM-IRRAS and XPS results show that azide groups are present at the SAM surfaces with different orientations and arrangements (isolated dipoles and antiparallel dipole–dipole interactions) depending on the deposition methods. It is important to note that if antiparallel dipole–dipole interactions occur, the most favorable orientation for the involved azide groups is certainly parallel to the surface, as shown in Scheme 1. Consequently, due to the surface selection rule of the PM-IRRAS, these azide groups do not contribute to the intensity of the ν_aN_3 band.

3.2. PM-IRRAS evaluation of click chemistry

It is now important to investigate the accessibility of these azide groups for further surface reactions. To explore this point, we examined the immobilization of an organic probe, 1-(but-3-yn-1-yloxy)-4-nitrobenzene **3** (Supporting information), bearing an alkyne function and a nitro substituent via CuAAC reaction (Scheme 1). The nitro substituent has been chosen since it is easily detected in the infrared region, from the antisymmetric (ν_aNO_2) and symmetric (ν_sNO_2) stretching

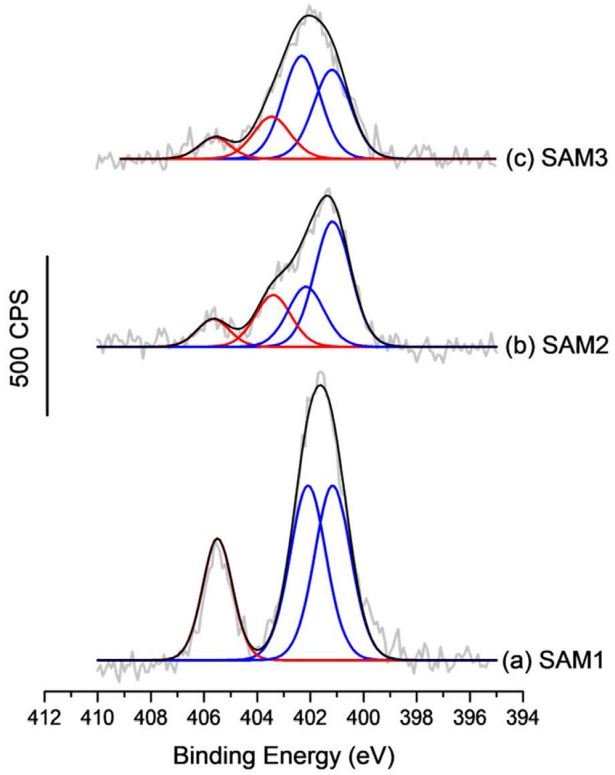

Fig. 2. High resolution XPS spectra of the N1s region for **SAM-N3** surfaces: a) post-functionalized **SAM1**, b) functionalized by immersion **SAM2** and c) functionalized by spin coating **SAM3**. The blue contributions at low Binding Energy are assigned to the electron enriched ($^{-}$N=) and neutral (=N-) nitrogen atoms, while the red contribution is assigned to the electron deficient (=N^{+}=) nitrogen atoms. (For interpretation of the references to colour in this figure legend, the reader is referred to the web version of this article.)

modes of the NO_2 moiety at 1515 and 1342 cm^{-1}, respectively. The CuAAC reaction was performed using a copper sulfate / sodium ascorbate catalytic system in a mixture of water and DMSO containing the organic probe.

The chemically modified surfaces have been characterized by PM-IRRAS. After the covalent immobilization of the nitro derivative *via* the click reaction (Fig. 3a), we observed the complete disappearance of the ν_aN_3 band at 2100 cm^{-1} on the **SAM1-NO2** spectrum associated with the appearance of new bands at 1608 (νC=C), 1594 (νC=C), 1499 (νC=C), 1515 (ν_aNO_2) and 1342 cm^{-1} (ν_sNO_2), related to the nitrophenyl moiety. The total disappearance of the ν_aN_3 band in the PM-IRRAS spectra clearly demonstrated the complete reaction of the azide groups on the surface with the acetylene compound and indirectly the successful formation of 1,2,3-triazole moiety on the monolayer. In addition, the region of methylene stretching modes does not reveal any degradation of the monolayer during the click reaction since the bands remained comparable in position and in intensity. The similar observations were obtained for **SAM2-NO2** and **SAM3-NO2** (Fig. 3b) revealing again the complete reactivity of the azide groups. However, these normalized spectra show that the intensity of the characteristic bands of the organic probe depends on the deposition method. To highlight this observation, the plot of the ν_aNO_2 intensity with respect to the ν_aN_3 intensity is presented in Supporting information (Fig. S6) for the three methods of deposition. This graph clearly shows that there is a linear dependence between the intensities of the azide band and those of the nitro band of the probe. The amount of nitro probe at the surface is directly correlated to the azide groups exhibiting a contribution on PM-IRRAS spectra (i.e. azide groups having a preferential vertical

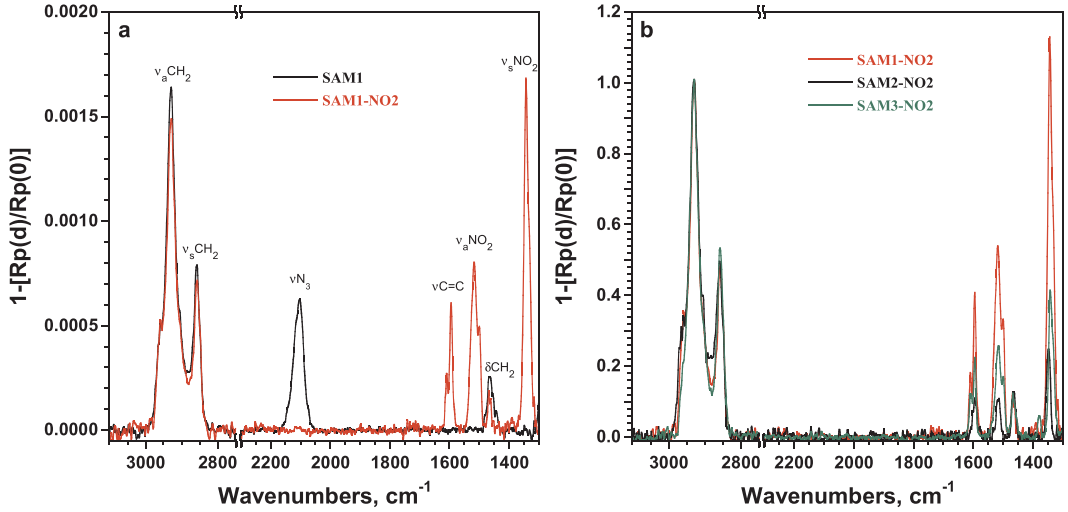

Fig. 3. a) Non normalized PM-IRRAS spectra before and after the click reaction with the nitro probe for the post-functionalized **SAM1**. b) Normalized PM-IRRAS spectra of SAMs after click reaction for the three methods of deposition in the 3100–1300 cm^{-1} spectral range.

orientation). This result seems to indicate that only these azide groups were accessible to react with the probe onto the surface.

3.3. Characterization of the azide reactivity by XPS

XPS spectrum of the triazole silylated compound **5** (Supporting information) was also measured in the N1s region to acquire spectral reference of the triazole group (Supporting information, Fig. S5b) and to compare it to the one of the azide compound **4**. As shown in Fig. S5b, XPS spectrum of the triazole compound **5** clearly shows the disappearance of the azide signal at high binding energy (~405 eV) associated with an enlargement of the main contribution centered at 401.5 ± 0.1 eV, that could be decomposed into three different peaks related to the three chemical environments of the three nitrogen atoms in the triazole ring [34]. Thus, XPS analyses were carried out for the three **SAM-N3** clicked with heptyne (Scheme 1) and compared to a direct grafting of **5**. The XPS spectra of these four samples, presented in Fig. 4 present the same overall N1s profile with a large and broad contribution centered between 401 and 402 eV, with no distinguishable signal at higher binding energy (ca 405–406 eV) related to azido groups with a preferential vertical orientation. In other words, all azido groups with a preferential vertical orientation have reacted *via* the click reaction, which is consistent with the disappearance of the azide bands observed by PM-IRRAS. As expected, the XPS spectrum of **SAM-H** (direct grafting of **5**), presented in Fig. 4a is very similar to the signal obtained for compound **5** (Supporting information, Fig. S5b). Considering the **SAM-N3** samples that underwent a click reaction, two different N1s profiles have been observed: **SAM1-H**, prepared by the post-functionalization method, displays N1s profile similar to the **SAM-H** sample with three contributions of equal weight. In this case, all azide groups seem to be clicked. On the contrary, for **SAM2-H** and **SAM3-H** samples, prepared by the direct grafting of the azido organosilane, the three contributions exhibit different weights from one to another. More precisely, the contribution at 403 eV, assigned to the central nitrogen atom ($=N^+=$) of azides in dipole–dipole interactions with neighboring azido groups, is still observed (a comparison of **SAM3** and **SAM3-H** is presented in Fig. S7). It has to be noticed that this population of azido groups involved in dipole–dipole interactions while lying parallel to the surface is not visible by PM-IRRAS analysis due to the surface selection rule. However, the XPS analysis clearly shows that this type of azides is not accessible to react by the click reaction. Strikingly, we can discriminate by XPS different kinds of azide groups and we have proven that the reactivity of azido groups dramatically

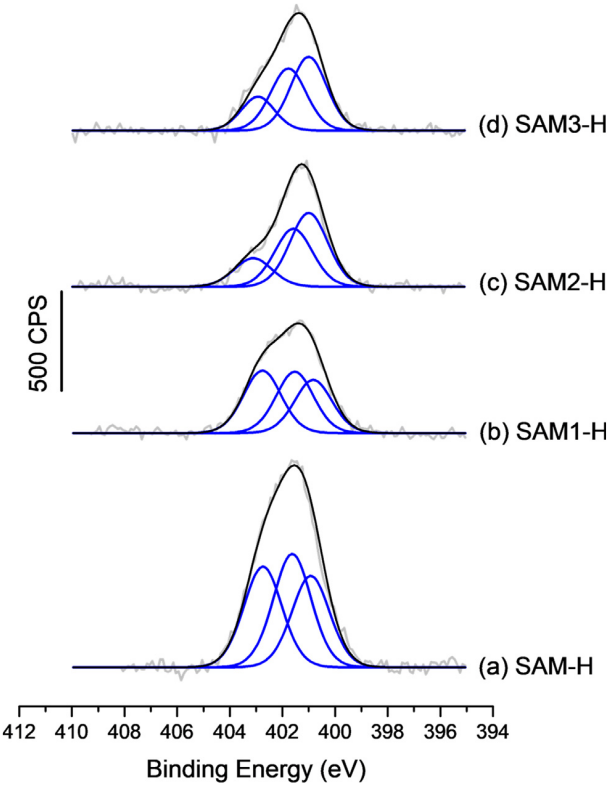

Fig. 4. High resolution XPS spectra of the N1s region for triazole SAMs obtained either directly or after click reaction of **SAM-N3** with heptyne: a) **SAM-H** (direct grafting of compound **5**), b) **SAM1-H** (post-functionalized from SAM-Br), c) **SAM2-H** (functionalized by immersion), and d) **SAM3-H** (functionalized by spin coating).

depends on their orientation in the monolayer. The click reaction is not total for **SAM2-H** and **SAM3-H** and only the portion of isolated azide with a preferential vertical orientation is reactive *via* the click reaction.

4. Conclusion

In the field of biosensors, biotechnology and biocatalysts the covalent immobilization of (bio)molecular species on solid supports

constitutes a great challenge to improve stability, reusability, and localization. Click chemistry is widely used to immobilize biomolecules on surfaces thanks to its high efficiency, ease of use and high yields. This study shows that the reactivity of the azido group on the surface with the alkyne in solution is closely related to the orientation of the azide. Indeed, the more the azide is vertically oriented the more it is accessible and reactive. The orientation of azido dipoles at the surface strongly depends on the method used to prepare the monolayer, and the post-functionalization method provides the best orientation of the azido groups for further reaction. This study demonstrates that it is possible to control the amount of reactive azide and consequently the amount of molecules immobilized on the surface after the click reaction by choosing the deposition method. Future work will focus on exploring the influence of the different deposition methods for new molecular architectures.

CRediT authorship contribution statement

Nisreen Al-Hajj: Investigation. **Yannick Mousli:** Investigation. **Antoine Miche:** Investigation. **Vincent Humblot:** Investigation, Formal analysis, Visualization. **Julien Hunel:** Visualization, Investigation. **Karine Heuzé:** Conceptualization. **Thierry Buffeteau:** Validation, Investigation, Writing - original draft, Writing - review & editing, Visualization. **Emilie Genin:** Supervision, Conceptualization, Writing - review & editing. **Luc Vellutini:** Supervision, Conceptualization, Writing - original draft, Writing - review & editing.

Acknowledgements

The authors acknowledge IMPC from Sorbonne University (Institut des Matériaux de Paris Centre, FR CNRS 2482) and the C'Nano projects of the Region Ile-de-France, for Omicron XPS apparatus funding. Financial support from "Consulat Général de France à Jérusalem" (NAH PhD grant), Bordeaux University and the CNRS are gratefully acknowledged.

[1] D. Samanta, A. Sarkar, Immobilization of bio-macromolecules on self-assembled monolayers: methods and sensor applications, Chem. Soc. Rev. 40 (2011) 2567–2592, https://doi.org/10.1039/C0CS00056F.
[2] P. Jonkheijm, D. Weinrich, H. Schöder, C.M. Niemeyer, H. Waldmann, Chemical strategies for generating protein biochips, Angew. Chem. Int. Ed. 47 (2008) 9618–9647, https://doi.org/10.1002/anie.200801711.
[3] V. Tjong, L. Tang, S. Zauscher, A. Chilkoti, Smart DNA interfaces, Chem. Soc. Rev. 4 (2014) 1612–1626, https://doi.org/10.1039/C3CS60331H.
[4] C.-J. Huang, Advanced Surface Modification Technologies for biosensors, in: K. Mitsubayashi, O. Niwa, Y. Ueno (Eds.), Chemical, Gas, and Biosensors for Internet of Things and Related Application, Elsevier Inc., 2019, pp. 65–86.
[5] Y. Rahm awan, L. Xu, S. Yang, Self-assembly of nanostructures towards transparent, superhydrophobic surfaces, J. Mater. Chem. A 1 (2013) 2955–2969, https://doi.org/10.1039/C2TA00288D.
[6] D.H. Dinh, L. Vellutini, B. Bennetau, C. Dejous, D. Rebière, E. Pascal, D. Moynet, C. Belin, B. Desbat, C. Labrugère, J.P. Pillot, Route to smooth silica-based surfaces decorated with novel self-assembled monolayers (SAMs) containing glycidyl-terminated very long hydrocarbon chains, Langmuir 2 (2009) 5526–5535, https://doi.org/10.1021/la804088d.
[7] I. Banerjee, R.C. Pangule, R.S. Kane, Antifouling Coatings: Recent Developments in Organisms, Adv. Mater. 23 (2011) 690–718, https://doi.org/10.1002/adma.201001215.
[8] S.K. Vashist, E. Lam, S. Hrapovic, K.B. Male, J.H.T. Luong, Immobilization of Antibodies and Enzymes on 3-Aminopropyltriethoxysilane-Functionalized Bioanalytical Platforms for Biosensors and Diagnostics, Chem. Rev. 11 (2014) 11083–11130, https://doi.org/10.1021/cr5000943.
[9] L.S. Wong, F. Khan, J. Micklefield, Selective Covalent Protein Immobilization: Strategies and Applications, Chem. Rev. 10 (2009) 4025–4053, https://doi.org/10.1021/cr8004668.
[10] S.P. Pujari, L. Scheres, A.T.M. Marcelis, H. Zuilhof, Covalent Surface Modification of Oxide Surfaces, Angew. Chem. Int. Ed. 53 (2014) 6322–6356, https://doi.org/10.1002/anie.201306709.
[11] S. Onclin, B.J. Ravoo, D.N. Reinhoudt, Engineering Silicon Oxide Surfaces Using Self-Assembled Monolayers, Angew. Chem. Int. Ed. 4 (2005) 6282–6304, https://doi.org/10.1002/anie.200500633.
[12] C. Haensch, S. Hoeppener, U.S. Schubert, Chemical modification of self-assembled silane based monolayers by surface reactions, Chem. Soc. Rev. 39 (2010) 2323–2334, https://doi.org/10.1039/B920491A.
[13] C.J. Pickens, S.N. Johnson, M.M. Pressnall, M.A. Leon, C.J. Berkland, Practical Considerations, Challenges, and Limitations of Bioconjugation via Azide-Alkyne Cycloaddition, Bioconjugate Chem. 29 (2018) 686–701, https://doi.org/10.1021/acs.bioconjchem.7b00633.
[14] D.M. Patterson, L.A. Nazarova, J.A. Prescher, Finding the right (bioorthogonal) chemistry, ACS Chem. Biol. 9 (2014) 592–605, https://doi.org/10.1021/cb400828a.
[15] A.C. Braun, M. Gutmann, T. Lühmann, L. Meinel, Bioorthogonal strategies for site-directed decoration of biomaterials with therapeutic proteins, J. Control. Release 273 (2018) 68–85, https://doi.org/10.1016/j.jconrel.2018.01.018.
[16] L. Nebhani, C. Barner-Kowollik, Orthogonal Transformations on Solid Substrates: Efficient Avenues to Surface Modification, Adv. Mater. 2 (2009) 3442–3468, https://doi.org/10.1002/adma.200900238.
[17] C.N. Sukenik, N. Balachander, Monolayer transformation by nucleophilic substitution: Applications to the creation of new monolayer assemblies, Langmuir 6 (1990) 1621–1627, https://doi.org/10.1021/la00101a001.
[18] H. Hoffmann, T. Lummerstorfer, Click Chemistry on Surfaces: 1,3-Dipolar Cycloaddition Reactions of Azide-Terminated Monolayers on Silica, J. Phys. Chem. B 108 (2004) 3963–3966, https://doi.org/10.1021/jp049601t.
[19] S. Prakash, T.M. Long, J.C. Selby, J.S. Moore, M.A. Shannon, "Click" Modification of Silica Surfaces and Glass Microfluidic Channels, Anal. Chem. 79 (2007) 1661–1667, https://doi.org/10.1021/ac061824n.
[20] S.-Y. Ku, K.-T. Wong, A.J. Bard, Surface Patterning with Fluorescent Molecules Using Click Chemistry Directed by Scanning Electrochemical Microscopy, J. Am. Chem. Soc. 13 (2008) 2392–2393, https://doi.org/10.1021/ja078183d.
[21] G. Qing, H. Xiong, F. Seela, T. Sun, Spatially Controlled DNA Nanopatterns by "Click" Chemistry Using Oligonucleotides with Different Anchoring Sites, J. Am. Chem. Soc. 132 (2010) 15228–15232, https://doi.org/10.1021/ja105246b.
[22] S. Zhang, J.T. Koberstein, Azide Functional Monolayers Grafted to a Germanium Surface: Model Substrates for ATR-IR Studies of Interfacial Click Reactions, Langmuir 28 (2012) 486–493, https://doi.org/10.1021/la203844v.
[23] A.C. Gouget-Laemmel, J. Yang, M.A. Lodhi, A. Siriwardena, D. Aureau, R. Boukherroub, J.-N. Chazalviel, F. Ozanam, S. Szunerits, Functionalization of Azide-Terminated Silicon Surfaces with Glycans Using Click Chemistry: XPS and FTIR Study, J. Phys. Chem. C 117 (2013) 368–375, https://doi.org/10.1021/jp309866d.
[24] R. Chisholm, J.D. Parkin, A.D. Smith, G. Hähner, Isothiourea-Mediated Organocatalytic Michael Addition-Lactonization on a Surface: Modification of SAMs on Silicon Oxide Substrates, Langmuir 32 (2016) 3130–3138, https://doi.org/10.1021/acs.langmuir.5b04686.
[25] S. Zheng, Q. Yang, B. Mi, Novel antifouling surface with improved hemocompatibility by immobilization of polyzwitterions onto silicon via click chemistry, Appl. Surf. Sci. 363 (2016) 619–626, https://doi.org/10.1016/j.apsusc.2015.12.081.
[26] M.C. Bertolino, A.M. Granados, Synthesis in situ of gold nanoparticles by a dialkynyl Fisher carbene complex anchored to glass surfaces, Appl. Surf. Sci. 383 (2016) 375–381, https://doi.org/10.1016/j.apsusc.2016.03.214.
[27] A.G. Marrani, E.A. Dalchiele, R. Zanoni, F. Decker, F. Cattaruzza, D. Bonifazi, M. Prato, Functionalization of Si(100) with ferrocene derivatives via « click » chemistry, Electrochim. Acta 53 (2008) 3903–3909, https://doi.org/10.1016/j.electacta.2007.10.051.
[28] S. Zhang, Y. Maidenberg, K. Luo, J.T. Koberstein, Adjusting the Surface Areal Density of Click-Reactive Azide Groups by Kinetic Control of the Azide Substitution Reaction on Bromine-Functional SAMs, Langmuir 30 (2014) 6071–6078, https://doi.org/10.1021/la501233w.
[29] A. Heise, M. Stamm, M. Rauscher, H. Duschner, H. Menzel, Mixed silane self assembled monolayers and their in situ modification, Thin Solid Films 327–329 (1998) 199–203, https://doi.org/10.1016/S0040-6090(98)00628-2.
[30] J. Böhmler, A. Ponche, K. Anselme, L. Ploux, Self-Assembled Molecular Platforms for Bacteria/Material Biointerface Studies: Importance to Control Functional Group Accessibility, ACS Appl. Mater. Interfaces 5 (2013) 10478–10488, https://doi.org/10.1021/am401976g.
[31] G.E. Fryxell, P.C. Rieke, L.L. Wood, M.H. Engelhard, R.E. Williford, G.L. Graff, A.A. Campbell, R.J. Wiacek, L. Lee, A. Halverson, Nucleophilic Displacements in Mixed Self-Assembled Monolayers, Langmuir 12 (1996) 5064–5075, https://doi.org/10.1021/la9506842.
[32] I. Alves, I. Kurylo, Y. Coffinier, A. Siriwardena, V. Zaitsev, E. Harté, R. Boukherroub, S. Szunerits, Plasmon waveguide resonance for sensing glycan-lectin interactions,

[33] X. Han, S. Bian, Y. Liang, K.N. Houk, A.B. Braunschweig, Reactions in Elastomeric Nanoreactors Reveal the Role of Force on the Kinetics of the Huisgen Reaction on Surfaces, J. Am. Chem. Soc. 136 (2014) 10553–10556, https://doi.org/10.1021/ja504137u.

[34] E.H. Chen, S.R. Walter, S.T. Nguyen, F.M. Geiger, Arylsilanated SiOx Surfaces for Mild and Simple Two-Step Click Functionalization with Small Molecules and Oligonucleotides, J. Phys. Chem. C. 116 (2012) 19886–19892, https://doi.org/10.1021/jp306437b.

[35] K. Barral, A.D. Moorhouse, J.E. Moses, Efficient Conversion of Aromatic Amines into Azides: A One-Pot Synthesis of Triazole Linkages, Org. Lett. 9 (2007) 1809–1811, https://doi.org/10.1021/ol070527h.

[36] M.S. Azam, S.L. Fenwick, J.M. Gibbs-Davis, Orthogonally Reactive SAMs as a General Platform for Bifunctional Silica Surfaces, Langmuir 27 (2011) 741–750, https://doi.org/10.1021/la1041647.

[37] Z. Li, C.N. Weeraman, J.M. Gibbs-Davis, Following the Azide-Alkyne Cycloaddition at the Silica/Solvent Interface with Sum Frequency Generation, ChemPhysChem 15 (2014) 2247–2251, https://doi.org/10.1002/cphc.201402161.

[38] L. Rouvière, Y. Mousli, I. Traboulsi, J. Hunel, T. Buffeteau, K. Heuzé, L. Vellutini, E. Genin, Hydrosilylation of Azide-Containing Olefins as a Convenient Access to Azidoorganotrialkoxysilanes for Self-Assembled Monolayer Elaboration onto Silica by Spin Coating, ChemistrySelect 3 (2018) 7333–7339, https://doi.org/10.1002/slct.201800858.

[39] G. London, G.T. Carroll, T.F. Landaluce, M.M. Pollard, P. Rudolf, B.L. Feringa, Light-driven altitudinal molecular motors on surfaces, Chem. Commun. (2009) 1712–1714, https://doi.org/10.1039/B821755F.

[40] P.K.B. Palomaki, P.H. Dinolfo, A Versatile Molecular Layer-by-Layer Thin Film Fabrication Technique Utilizing Copper(I)-Catalyzed Azide − Alkyne Cycloaddition, Langmuir 26 (2010) 9677–9685, https://doi.org/10.1021/la100308j.

[41] P. Paoprasert, J.W. Spalenka, D.L. Peterson, R.E. Ruther, R.J. Hamers, P.G. Evans, P. Gopalan, Grafting of poly(3-hexylthiophene) brushes on oxides using click chemistry, J. Mater. Chem. 20 (2010) 2651–2658, https://doi.org/10.1039/B920233A.

[42] S. Pookpanratana, I. Savchenko, S.N. Natoli, S.P. Cummings, L.J.J. Richter, W.F. Robertson, C.A. Richter, T. Ren, C.A. Hacker, Attachment of a Diruthenium Compound to Au and SiO2/Si Surfaces by “Click” Chemistry, Langmuir 30 (2014) 10280–10289, https://doi.org/10.1021/la501670c.

[43] R. Vos, C. Rolin, J. Rip, T. Conard, T. Steylaerts, M.V. Cabanilles, K. Levrie, K. Jans, T. Stakenborg, Chemical Vapor Deposition of Azidoalkylsilane Monolayer Films, Langmuir 34 (2018) 1400–1409, https://doi.org/10.1021/acs.langmuir.7b04011.

[44] M.A. Pellow, T.D. Stack, C.E.D. Chisey, Squish and CuAAC: Additive-Free Covalent Monolayers of Discrete Molecules in Seconds, Langmuir 29 (2013) 5383–5387, https://doi.org/10.1021/la400172w.

[45] J.C. Niehaus, M. Hirtz, M.K. Brinks, A. Studer, H. Fuchs, L. Chi, Patterning of Functional Compounds by Multicomponent Langmuir − Blodgett Transfer and Subsequent Chemical Modification, Langmuir 26 (2010) 15388–15393, https://doi.org/10.1021/la102881r.

[46] T. Buffeteau, B. Desbat, J.-M. Turlet, Polarization Modulation FT-IR Spectroscopy of Surfaces and Ultra-thin Films: Experimental Procedure and Quantitative Analysis, Appl. Spectrosc. 45 (1991) 380–389, https://doi.org/10.1366/0003702914337308.

[47] M.A. Ramin, G. Le Bourdon, N. Daugey, B. Bennetau, L. Vellutini, T. Buffeteau, PM-IRRAS Investigation of Self-Assembled Monolayers Grafted onto SiO2/Au Substrates, Langmuir 27 (2011) 6076–6084, https://doi.org/10.1021/la2006293.

[48] T. Buffeteau, B. Desbat, D. Blaudez, J.-M. Turlet, Calibration Procedure to Derive IRRAS Spectra from PM-IRRAS, Spectra, Appl. Spectrosc. 54 (2000) 1646–1650, https://doi.org/10.1366/0003702001948673.

[49] J.H. Scofield, Hartree-Slater subshell photoionization cross-sections at 1254 and 1487 eV, J. Electron. Spectrosc. Relat. Phenom. 8 (1976) 129–137, https://doi.org/10.1016/0368-2048(76)80015-1.

[50] H.-G. Steinrück, J. Will, A. Magerl, B.M. Ocko, Structure of n-Alkyltrichlorosilane Monolayers on Si(100)/SiO_2, Langmuir 31 (2015) 11774–11780, https://doi.org/10.1021/acs.langmuir.5b03091.

[51] C.-K. Liang, G.V. Dubacheva, T. Buffeteau, D. Cavagnat, P. Hapiot, B. Fabre, J.H.R. Tucker, D.M. Bassani, Reversible Control over Molecular Recognition in Surface-Bound Photoswitchable Hydrogen-Bonding Receptors: Towards Read–Write–Erase Molecular Printboards, Chem. Eur. J. 19 (2013) 12748–12758, https://doi.org/10.1002/chem.201301613.

[52] M.J. Dignam, S. Mamiche-Afara, Determination of the spectra of the optical constants of bulk phases *via* Fourier transform ATR, Spectrochim. Acta, Part A 44 (1988) 1435–1442, https://doi.org/10.1016/0584-8539(88)80195-8.

[53] E. Siurdyban, T. Brotin, K. Heuzé, L. Vellutini, T. Buffeteau, Immobilization of Cryptophane Derivatives onto SiO_2/Au and Au Substrates, Langmuir 30 (2014) 14859–14867, https://doi.org/10.1021/la5039156.

[54] G.T. Carroll, G. London, T. Fernandez Landaluce, P. Rudolf, B.L. Feringa, Adhesion of Photon-Driven Molecular Motors to Surfaces *via* 1,3-Dipolar Cycloadditions: Effect of Interfacial Interactions on Molecular Motion, ACS Nano 5 (2011) 622–630, https://doi.org/10.1021/nn102876j.

[55] Z. Xiao, C. Cai, A. Mayeux, A. Milenkovic, The First Organosiloxane Thin Films Derived from SiCl3-Terminated Dendrons. Thickness-Dependent Nano- and Mesoscopic Structures of the Films Deposited on Mica by Spin-Coating, Langmuir 18 (2002) 7728–7739, https://doi.org/10.1021/la026001h.

[56] V. Vikrant, R. Städler, N.D. Spencer, Effect of Leaving Group on the Structures of Alkylsilane SAMs, Langmuir 30 (2014) 14824–14831, https://doi.org/10.1021/la503739j.

[57] J.P. Collman, N.K. Devaraj, T.P.A. Eberspacher, C.E.D. Chidsey, Mixed Azide-Terminated Monolayers: A Platform for Modifying Electrode Surfaces, Langmuir 22 (2006) 2457–2464, https://doi.org/10.1021/la052947q.

[58] G. Zorn, L.-H. Liu, L. Árnadóttir, H. Wang, L.J. Gamble, D.G. Castner, M. Yan, X-ray Photoelectron Spectroscopy Investigation of the Nitrogen Species in Photoactive Perfluorophenylazide-Modified Surfaces, J. Phys. Chem. C. 118 (2014) 376–383, https://doi.org/10.1021/jp409338y.